

Contents lists available at ScienceDirect

# **Applied Energy**

journal homepage: www.elsevier.com/locate/apenergy





# An experimental and numerical investigation of novel solution for energy management enhancement in data centers using underfloor plenum porous obstructions

Mohammad I. Tradat<sup>a,\*</sup>, Yaman "Mohammad Ali" Manaserh<sup>a,\*</sup>, Bahgat G. Sammakia<sup>a</sup>, Cong Hiep Hoang<sup>a</sup>, Husam A. Alissa<sup>b</sup>

#### HIGHLIGHTS

- Novel approach using porous partitions is introduced for improving overall data center energy efficiency.
- The effect of partitions on data center performance metrics is evaluated.
- Practical measures for reducing airflow non-uniformity is investigated to reduce energy losses.
- Parametric study for investigating the partitions geometry impact on the Supply heat index is conducted.

#### ARTICLE INFO

# Keywords: Data center Thermal management Energy efficiency Computational fluid dynamics Airflow management

#### ABSTRACT

This investigation focuses on improving the airflow distribution in data centers. In many data centers vortices form in the plenum during operations. These vortices cause spatial and temporal non-uniformities and may give rise to hot regions in the data center which in turn impacts performance and reliability of the IT equipment. The current study identifies a novel approach using porous partitions in the plenum and demonstrates a significant generalized approach that is easily adoptable in existing and future data centers. For improving the overall data center energy efficiency and the cooling system effectiveness by eliminating a critical source of inefficiency. The results of quantitative and qualitative analyses of the underfloor plenum pressure field, perforated tiles airflow rate, and air temperature at the rack intake side with and without partitions are presented. Different data center configurations are studied using physics-based experimentally validated Computational Fluid Dynamics (CFD) model. The CFD model results showed that the partitions eliminated the presence of vortices in the underfloor plenum and thus enabled a more uniform pressure distribution and tile airflow delivery. Regarding rack inlet temperature, the results showed that the partitions significantly improved the air temperature at the rack inlet. Finally, a geometrical parametric study is performed. An ideal design is and demonstrated to improve the Supply Heat Index (SHI) by about 10%, while the amount of IT equipment that exceeded the ASHRAE recommended supply air temperature (SAT) was reduced by about 40%, and the floor leakage was cut in half.

# 1. Introduction

As the world's energy demands continuously increase [1], so too does the search for energy efficiency enhancements to power consuming systems, like data centers. Data centers represent the information backbone of an increasingly digitalized world. The demand for their services has been rising rapidly. Data-intensive technologies, such as

artificial intelligence, smart and connected energy systems, distributed manufacturing systems, and autonomous vehicles promise to increase demand even further. Consequently, data center energy consumption has grown substantially [2]. Data centers are energy intensive enterprises, accounting for 1.3% of electricity usage worldwide [3], 30–50% of which is consumed by their cooling systems [4]. These numbers have prompted researchers to investigate energy saving opportunities and reliability concerns for data center cooling systems. There are various

E-mail addresses: mtradat1@binghamton.edu (M.I. Tradat), yyaseen1@binghamton.edu (Y.".A. Manaserh).

<sup>&</sup>lt;sup>a</sup> Departments of Mechanical Engineering, ES2 Center, Binghamton University-SUNY, NY, USA

<sup>&</sup>lt;sup>b</sup> Microsoft Redmond, WA, USA

<sup>\*</sup> Corresponding authors.

Vomen	clature	$ au_{ m ij}$	Stress tensor	
		Φ	Dissipation function	
$C_{1\varepsilon}, C_{2\varepsilon}$	$C_{\mu}$ Coefficients in eqns. (5) and (6)			
F	Body forces	Abbreviations		
FUI	Flow Uniformity Index	CFD	Computational Fluid Dynamics	
G	Generation of turbulent kinetic energy	CFM	Cubic Feet per Minute	
k	Kinetic energy	CRAC	Computer room air conditioning	
<b>k</b> *	Thermal conductivity	CRAH	Computer Room Air Handler	
'n	Mass flow rate	DC	Data center	
P	Pressure	HAC	Hot Aisle Containment	
		IT	Information technology	
Q	Heat flow rate	RANS	Reynolds averaged Navier-Stokes	
S	Volumetric heat generation	RAT	Return Air Temperature	
SAT	Supply air temperature	RHI	Return Heat Index	
$S_k, S_{\varepsilon}$	Source terms	SHI	Supply Heat Index	
Γ	Temperature	SLTBs	Server lower-side terminal baffles	
1	Velocity	UFB	Underfloor baffles	
$Y_{M}$	Fluctuating dilation in compressible turbulence			
3	Rate of turbulent kinetic energy dissipation	Subscrip	ts	
ı	Dynamic viscosity	В	Buoyancy force	
$u_t$	Turbulent viscosity	eff	Effective	
9	Fluid density			
$\sigma_k, \sigma_{\varepsilon}$	Turbulent Prandtl numbers			

cooling techniques being adapted in data centers, two common ones being liquid cooling [5,6] and two-phase cooling [7,8]. However, when it comes to the most reliable, well developed, and widespread cooling technique, air cooling takes the lead.

J. Cho and Y. Kim [9] presented an analytical approach to evaluate and optimize data center energy usage considering different geographical locations and used cooling systems. The authors studied four regions and examine the energy evaluation using energy model tool. They showed that data center's energy efficiency is highly dependent on the location on the planet and the deployed cooling system and infrastructure. An experimental and system level modeling were used by M. T-Evans et al. [10] to investigate the impact of cold air bypass the IT equipment on DCs energy consumption. The investigation performed by addressing the effect of leakage paths of server racks and experimentally quantified. Then, a system level model was developed and used to predict the impact of cold air bypass on each component power of the DC. The authors define guidelines to minimize the energy losses due to bypass through practical measures on the leakage paths and racks pressure differentials. B. Fakhim et al. [11] proposed and examined a few practical design and remedial solutions to enhance cooling effectiveness and to reduce the cooling system power requirements, Their investigation included the CRAC's layout, blank spaces beside the racks, cold-aisle containment, and an airflow distribution system with ceiling return. R. Gupta et al. [12] introduced a methodology to determine the exergy loss in the data center's different components, which was done by combining the computational fluid dynamics simulation with thermodynamic energy and exergy balances. While, L. S-Lianca et al. [13] compared two different approaches for Exergy Destruction (direct and indirect) using sets of data produced numerically through a commercial Finite Volume based software 6SigmaDX<sup>TM</sup> to model the airside behavior in an operational data center. The tests were performed for both simplified and actual cases. Their results revealed that both approaches worked well. Furthermore, the Exergy Destruction shows significant sources of irreversibility in the airside and the energy consumption can be improved by eliminating these sources in legacy data centers.

X. Yuan et al. [14] studied a tilted server placement in racks. Results showed that installing servers with a  $30^\circ$  tilted angle enhanced the cooling efficiency and lowered the maximum rack temperature by  $3.3~^\circ$ C. Y. Liu et al. [15] showed that a potential energy savings of up to

39.55% for the whole year can be achieved by integrating the data center cooling unit with a rotary booster and compressor. H. Cheung et al. [16] presented and developed equipment level power consumption model, which can be used for real time assessment of energy system simulation in data centers. Their results showed that the proposed model works well in simulating the IT power changes under dynamic operating conditions. J. Li et al. [17] introduced a new indicator to quantify data centers energy performance as an alternative of the commonly used metric; Power Usage Effectiveness (PUE); the authors proposed the use of a coefficient (COPUE) that considers the impacts of different climate conditions on data centers performance. Therefore, data centers energy consumption comparison can be independent from the geographical location and time of the year. Yann et al. [18] introduced and analyzed a new concept of an in-rack-cold-aisle (IR-CA) system. They studied seven different rack intake cross sectional areas with an additional partition plane placed at rack inlet. Their results revealed the optimal thermal distribution was obtained for the IR-CA case with partition plane among the rest studied cases.

A. Khalaj and S. Halgamuge [19] introduced a summary of the literature on data centers thermal management. The authors reviewed most of the published work related to air and liquid cooled DCs. They focused on the inherent sources of inefficiencies and the techniques for improving DCs energy efficiency. Furthermore, H. Lu et al. [20] presented a review on the effects of underfloor plenum geometries on the airflow distribution in data centers considering different configurations such as cold aisle, hot aisle containment and vertical exhaust duct systems. Also, the authors summed up a major portion of numerical and experimental research upon the underfloor air distribution (UFAD). Recently, C. Jin et al. [21] surveyed and provided an overview of server's power consumption models in DCs environment. While P. Huang et al. [22] filled the gap by introducing a review that integrated between the energy supply side (upstream green energy) and the reuse of waste heat as well as the renewable energy and advanced control techniques in data centers. Finally, Gong et al [23] introduced a comprehensive review of the state of the art of thermal performance evaluation in data centers. They focused on metrics characteristics and application level (room, row, rack and server levels). The authors discussed major metrics advantages and limitations and proposed an evaluation criteria for data centers designers and operators for using the most appropriate indices for data center optimization.

Further studies concentrated on the flow field and pressure distribution in the underfloor plenum [24-27], since they have a major influence on the amount and uniformity of the cooling air delivered through the perforated tiles. Shrivastava et al. [24] built a multi-scale 3-D model of an air-cooled data center, including an under-floor plenum to improve the data centers cooling system efficiency, and hence energy consumption. Khalili et al. [25] conducted a parametric simulation of three types of floor tiles with different open area, opening geometry, and understructure considered. They used an experimentally validated detail model of tiles implemented in CFD simulations to address the impact of tile design on the cooling of IT equipment in both open and enclosed aisle configuration. Zhang et al. [26] investigated the influence of different raised floor heights on airflow distribution for three different configurations (HA-CA, CAC, and HAC) using commercial CFD software. Song Z. [27] numerically studied and identified the fan assisted perforations limits. The author investigated two different aspects of data center configuration, namely; a fan-assisted tile and a fan to tile distance. His results showed that the fan assisted tile is viable to efficiently manage data centers. More in-depth studies on the presence of underfloor blockages related to data center infrastructure (chiller pipes, cables, and conduits) received the interest of many researchers. Some researchers' results [28-32] indicated that the existence of underfloor obstructions could have a negative influence the airflow delivery and so the cooling system performance. VanGilder and Schmidt [28] analyzed over 240 CFD models to estimate the effects of different parameters on the uniformity of tile airflow. The results showed that tile type and the existence of underfloor obstructions have the greatest influence, among other design recommendations; the authors recommended keeping the outlet region of the cooling unit free of pipes and cables in order to gain uniform tile airflow. Bhopte et al. [29,30] characterized the impact of under-floor blockages on DC performance. They established guidelines in the form of Plenum Color Code. Moreover, they experimentally validated the guidelines on a different DC and presented a comparison between numerical and experimental results. The results showed the severe impact of critically located blockages, which reduced the airflow rate of supply tiles by 19%. Alissa et al. [31] numerically studied the thermal and flow effects of under-floor obstructions in a DC. Open and contained environments were considered. For the open case, they compared between a parallel and perpendicular distribution of blockages in both critical and safe locations. A perpendicular distribution of blockages in a critical location and improper distribution of infrastructure blockages was found to have severe effects on the hydrodynamic and thermal behavior, which is due to a reduction of the air feed to IT equipment and operating points. Seven CFD models were built by Fulpagare et al. [32] to investigate the effect of underfloor blockages, among other factors, on the CRAH airflow rates and distribution. The results showed that underfloor obstructions could reduce the airflow rate as much as 80% and increase exit air temperature by 2.5 °C. In contrast to the previous results, some researchers found that the presence of a plenum obstruction could be beneficial [33,34]. Based on this, further research on deliberated obstructions that are selectively installed in the underfloor plenum has been conducted. These obstructions included thin partitions [35], T-shaped underfloor air duct network [36], and inclined underfloor baffles [37]. Lu and Zhang [38] numerically investigated 6 different local partitions models to analyze their effect on local hot spot formation. In another study [39] they investigated the effect of plenum height, tiles perforation, cooling units arrangement and operating conditions such as temperature and air volume on the thermal performance of data centers. They reported that data center geometry can significantly enhance data center thermal performance. Furthermore, the authors reported a reduction in inlet and outlet air temperature by 1.7-2.9 °C by means of inclined partitions to create plenum gradient cross-section.

In a legacy air-cooled and raised floor data center, the Computer Room Air Handler (CRAH) supplies cold air into the underfloor plenum, which distributes the cooling airflow to cold aisles and then to the computer racks through perforated tiles. Therefore, the performance of the cooling system is influenced by an improved airflow distribution, which is driven by many design factors, such as underfloor plenum geometry, CRAH's nominal supply/location, perforated tiles openness, etc. The cooling airflow rate through the perforated tiles must satisfy the demand of nearby IT equipment to ensure reliability and functionality as the cooling air emerges from the tiles, the velocity of horizontal flow in the plenum decreases and hence the pressure increases. These pressure variations in the horizontal plane under the raised floor lead to non-uniform flow rates from different tiles. The furthest tile from the perimeter CRAH usually gets the largest amount of air since room size plays a vital role [36].

Another factor that will cause a maldistribution of the flow field is the formation of vortices. In the previous work [40], the authors presented a measured dataset of the tiles flow rate in the ES2 data center laboratory located at State University of New York at Binghamton, which shows a variation among the vertical distance from the cooling unit. This non-uniformity is related to the presence of a vortex that caused a pressure wake under the raised floor. On that account, the amount and uniformity of the delivered cooling air are mainly affected by flow field and pressure distribution in the underfloor plenum, which is considered a very important element amongst other challenging tasks in data centers. Considering the underfloor plenum depth, modified perforated tile open area, and the selectively located partitions and airdirectors under the raised floor will influence the plenum pressure field and thus more uniform tiles delivery. The key to modifying the airflow rates through perforated tiles is to influence the pressure field in the underfloor plenum. The presented partition influences the plenum pressure field uniformity and thus tiles airflow rates by eliminating the vortices in the plenum under the cold aisle. The authors numerically studied the effect of underfloor air-directors on the airflow uniformity by comparing different layouts and locations. The results showed that a more uniform airflow field was achieved by placing the partitions directly under the cold aisles. As an extension of the author's previous work, this study aims to take the former conclusion further and investigate the partitions' benefit on energy efficiency, flow, and pressure fields by implementing them in a real data center environment. Subsequently, a novel approach for implementing beneficial partitions in the underfloor plenum was introduced. What distinguishes these deliberate underfloor plenum partitions from the ones that have been investigated before is that these partitions do not limit the flexibility of moving the cold aisle and cabinets around the data center, in fact, they can be easily adopted in existing and future data centers. Moreover, these partitions do not focus on guiding the airflow to the cold aisle, instead, it focuses on eliminating the source of maldistributions that causes the airflow delivery non-uniformity such as vortices. Perforated tiles airflow delivery non-uniformity was proven to play a vital role in lowering the energy efficiency of data centers [34]. This can be attributed to the fact airflow delivery non-uniformity results in under-provisioning some spots in the cold aisle which in turn promotes the hot air recirculation in these locations and hence, increasing the mixing between the hot and cold streams.

For many years, Plenum vortices are identified as a significant energy inefficiency source in data centers while left with no clear practical solution. Therefore, we are proposing a simple and passive solution for filling this knowledge gap. The essential contribution of this study is that it demonstrates an impressive, generalized approach for eliminating the underfloor plenum vortices by using porous obstructions. To the best of the authors' knowledge, this solution has never been introduced or discussed in the literature before. The functionality of these partitions was verified experimentally, where deploying them showed an increment in the amount and uniformity of airflow delivery. Moreover, the impact of installing these partitions on the overall data center performance was exposed by exploiting an experimentally validated CFD model. Numerical results showed an improvement in the cooling system energy efficiency accommodated with lower floor leakage and reduction

of the number of IT equipment that operates under hazardous conditions when the partitions were deployed.

The paper is structured as follows. First, the physical domain is described, and the experimental results are presented in alignment with the numerical results. The description provides details about the data center facility used for testing, including aisles/tiles, available cooling, rack power density, etc. This is followed up by the design and setup of experiments as well as a description of the instruments used for measuring airflow, pressure, and temperature. Next, the numerical model is described in detail, including the selected grid generation criteria, governing equations, a grid independency study, and the model's validation. Finally, visualizations for the numerical and experimental results are presented and discussed.

#### 2. Methodology

# 2.1. Data center description and operating conditions

The data center laboratory profiled in the center for Energy-Smart Electronic Systems (ES2) is located at the State University of New York at Binghamton. The data center consists of five aisles named A, B, C, D and E, where aisle B is out of duty. A traditional arrangement of hot aisle/cold aisle is used in the laboratory. The data center has a variable distance from one cold aisle center to the next cold aisle center (aisle pitch). The aisle pitch varies between 7 and 9 raised floor (0.61 m  $\times$  0.61 m) panels. An overhead map view of the data center lab is shown in Fig. 1. Data center specifications, operating conditions, parameters, settings, and involved equipment are summarized in Table 1.

In this data center, the rack power density varies between racks. In addition, the perforated tiles have a dissimilar open area ratio. Appendix

**Table 1**Data center specifications and operating conditions.

Items	Description	Value
Room	Area	215.75 m <sup>2</sup>
	Height	4.37 m
	Raised floor height	0.914 m
	Total number of perforated Tiles	45
	Perforated tile dimensions	$(0.61 \times 0.61) \text{ m}$
	Number of racks	53
Total IT load		120 kW
CRAHs	Number of CRAHs	2
	SAT	18.8 °C
	Nominal cooling capacity	399 kW
	CRAH 1 maximum flow rate	$7.79 \text{ m}^3/\text{s}$
	CRAH 2 maximum flow rate	$8.165 \text{ m}^3/\text{s}$

A shows the details of racks power density and perforated tiles openness for each aisle. It can be noted from Appendix A that the perforated tile open area varies significantly and justifies the substantial variation in the flowrate delivered by each tile, which is further discussed in the following sections.

#### 2.2. Experimental setup

For ease of deployment, tiles measuring (0.61  $\times$  0.61) m with an open area of 22% were chosen as the partition to be installed in the plenum. These tiles are no longer called perforated tiles, instead they are referred to as partitions to distinguish them from the ones installed in the cold aisle. The partitions were only implemented under aisles C and D, as shown in Fig. 2 (a and b). These aisles were chosen because they are the main aisles in the ES2 data center and because the author's

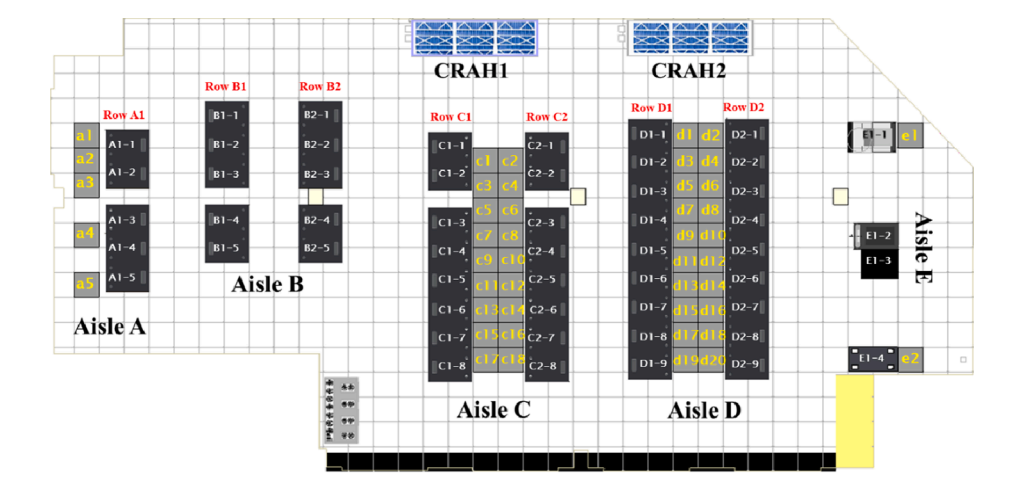
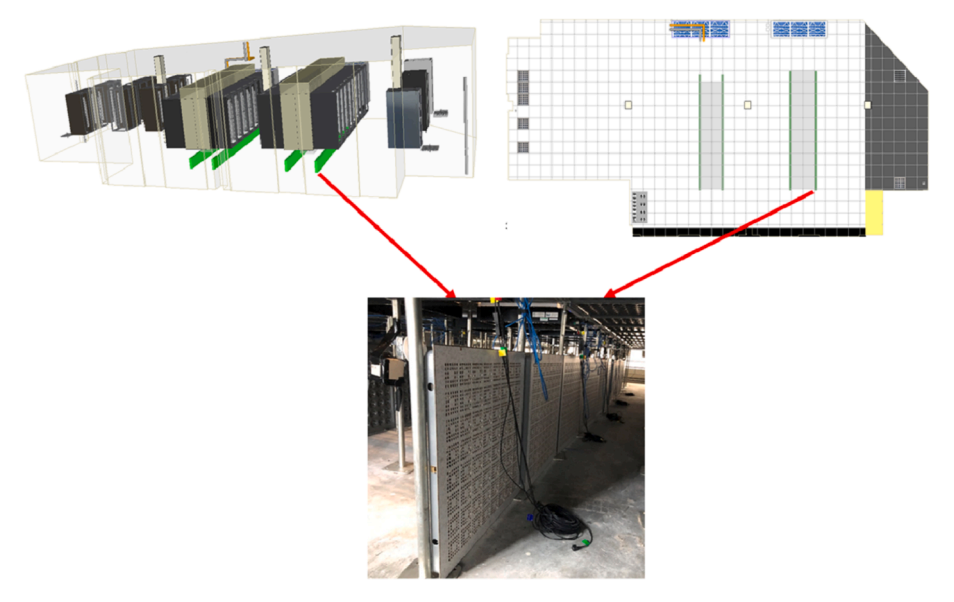




Fig. 1. Schematic for the ES2 data center.



(a) Partitions' installation.





(c) Flow hood.

(b) Perforated tiles.

Fig. 2. Location and Installation manner of partitions.

previous study [40] showed that they are the only ones that are exposed to the effect of plenum vortices.

The experiments were realized for four scenarios. In scenario 1, both CRAH units operated at 100% fan speed and no partitions were included. In scenario 2, both CRAH units operated at 100% fan speed and partitions were installed. In scenario 3, CRAH 1 was turned off while CRAH 2 operated at 100% fan speed and no partitions were included. Finally, in scenario 4, operating conditions resembled scenario 3, except that partitions were included. Table 2 summarizes the four scenarios.

A flow hood (ADM-850 L) multimeter (shown in Fig. 2 (c)) was used

 Table 2

 Experimental conditions for each scenario.

Scenario name	CRAH 1	CRAH 2	Partitions
Scenario 1	On	On	Not installed
Scenario 2	On	On	Installed
Scenario 3	Off	On	Not installed
Scenario 4	Off	On	Installed

to report the airflow rate of each perforated tile in the data center (locations are shown in Fig. 1 above) with a measurement accuracy of  $\pm 3\%$  of reading  $\pm 7$  CFM from 100 to 2000 CFM as reported by vendor technical manual. The device was equipped with an electronic micrometer to compensate the additional flow impedance by the hood. The airflow balance provided a backpressure airflow measurement, therefore the error caused by the hood was eliminated. Flowrate results were the average value of five measured flowrate values for each perforated tile, which was done to improve the reliability and obtain more accurate experimental results.

The purpose of this experiment was to prove the perforated partitions concept. The experiment considered the flowrate distribution through the perforated tiles with and without the perforated partitions. Further investigations were carried out using numerical simulation.

## 2.3. Numerical simulation

• Data center model

A CFD model that replicated the ES2 data center was developed using the commercial computational fluid dynamics (CFD) of 6SigmaRoom. This CFD code is intended for designing and operating data centers. It contains vast verified vendor libraries for different components in data centers, which made it easier to validate this model. After first validating the CFD model with the experimental results, the model was then used to visualize the effect of partitions on flow and pressure fields in the plenum and further investigate the benefits of partitions. The model was also used to run parametric studies that inspected the effect of partition geometry on the airflow delivered by the tiles.

# • Grid generation

Grid generation plays a vital role in controlling the accuracy of the simulation results. Thus, a proper grid quantity and quality should be considered when constructing the grid. In this study, a hex structured mesh was employed. Using flow aligned cubic hex cells provided the clear advantage of guaranteeing the grid quality and eliminating the typical issues of tetrahedral mesh, which are the aspect ratio and skewness [41]. To verify the appropriate number of grids, a grid independence study was executed, as illustrated in Fig. 3. After that, the chosen number of grids was selected to ensure that the results variation while increasing the mesh number is kept minimal.

It can be seen from Fig. 3 that when the grid number exceeded 17.4, the value of the highest perforated tile flow delivery rate no longer changed. Therefore, a grid number of 17.4 million was chosen to make a compromise between the computational time and the accuracy of results. Fig. 4 shows the grid generation for the data center.

#### · Governing equations and turbulence model

The conservation of mass, momentum, and energy governing equations are given as follows:

$$\frac{\partial \rho}{\partial t} + \frac{\partial (\rho \mathbf{u}_i)}{\partial \mathbf{x}_i} = 0 \tag{1}$$

$$\frac{\partial (\rho u_i)}{\partial t} + \frac{\partial (\rho u_i u_j)}{\partial x_i} = -\frac{\partial P}{\partial x_i} + \frac{\partial \tau_{ij}}{\partial x_j} + F_i \tag{2}$$

$$\frac{\partial (\rho E)}{\partial t} + \frac{\partial (u_{m}(\rho E + P))}{\partial x_{m}} = \frac{\partial}{\partial x_{j}} \left( k_{eff} \frac{\partial T}{\partial x_{j}} \right) + \Phi + S \tag{3}$$

where,  $\rho$ ,u<sub>i</sub>, P, k, T, and  $\tau$ <sub>ij</sub> represent the fluid density, velocity component, pressure, thermal conductivity, temperature, and stress tensor,

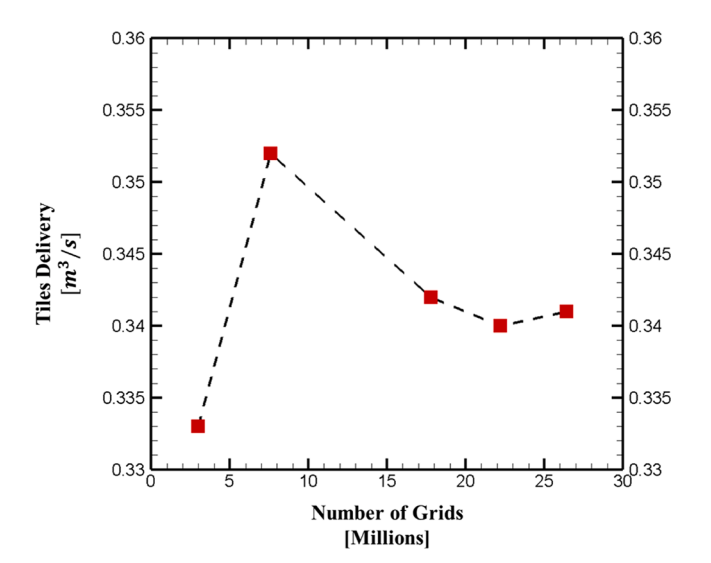


Fig. 3. Grid sensitivity analysis.

respectively. Next, $F_i$  represents the body forces,  $\Phi$  is the dissipation function, and S is the volumetric heat generation. Regarding the turbulence model, the standard k- $\epsilon$  turbulence model was selected to simulate the flow field through a coupling with RANS equations. This turbulence model was selected according to the literature, which has confirmed the feasibility of employing the standard k- $\epsilon$  turbulence model to DCs [42–44]. The governing equation of the standard k- $\epsilon$  turbulence model for calculating the turbulent kinetic energy k and its rate of dissipation  $\epsilon$  are [45–47]:

$$\frac{\partial (\rho k)}{\partial t} + \frac{\partial (\rho k u_i)}{\partial x_i} = \frac{\partial}{\partial x_j} \left[ \left( \mu + \frac{\mu_t}{\sigma_k} \right) \frac{\partial k}{\partial x_j} \right] + G_k + G_b - \rho \varepsilon - Y_M + S_K \tag{4} \label{eq:delta_total_eq}$$

$$\frac{\partial(\rho\varepsilon)}{\partial t} + \frac{\partial(\rho\varepsilon u_{i})}{\partial x_{i}} = \frac{\partial}{\partial x_{j}} \left[ \left( \mu + \frac{\mu_{t}}{\sigma_{\varepsilon}} \right) \frac{\partial\varepsilon}{\partial x_{j}} \right] + C_{1\varepsilon} \frac{\varepsilon}{k} (G_{k} + C_{3\varepsilon}G_{b}) - \rho C_{2\varepsilon} \frac{\varepsilon^{2}}{k} + S_{\varepsilon}$$

$$(5)$$

where,  $\mu$  and  $\mu_t$  represent the dynamic viscosity and turbulent viscosity, respectively. Turbulent viscosity is calculated using  $\mu_t = \rho C_\mu \frac{k^2}{\varepsilon}$ . Then,  $c_{1\varepsilon}$ ,  $c_{2\varepsilon}$ , and  $c_\mu$  are adjustable constants and their values are 1.44, 1.92, and 0.09, respectively. Next,  $\sigma_k$  and  $\sigma_\varepsilon$  are turbulent Prandtl numbers for the turbulent kinetic energy and its dissipation rate, respectively. Based on the experimental derivation,  $\sigma_k = 1$ , and  $\sigma_\varepsilon = 1.3$ . Next,  $G_k$ , and  $G_b$  denote the generation of turbulent kinetic energy that arises due to mean velocity gradients and buoyancy, respectively. Next,  $Y_M$  represents the fluctuating dilation in compressible turbulence that contributes to the overall dissipation rate. Finally,  $S_k$ , and  $S_\varepsilon$  are source terms.

The following assumptions were made while running the simulations:

- (a) Steady state conditions are achieved.
- (b) Air is incompressible and has constant properties.
- (c) The impacts of wall roughness and gravity are negligible.
- (d) Outer walls are adiabatic (floor and ceiling).
- (e) Finally, since there are few infrastructure blockages (chiller pipes) the underfloor plenum is considered empty.
  - Model validation

The physics based CFD model of the ES2 data center research laboratory was developed and refined over years to quantify the confidence and predictive accuracy of the model under the supervision of the used CFD commercial software developer [40]. Moreover, to ascertain the model accuracy, a validation experiment was conducted and the CFD model results compared to the experimental ones, the comparison considered tile flowrate delivery and temperature measurements. The details of the validation experiment operating conditions are provided in Table 3 for the validation experiment, SynapSense<sup>TM</sup> sensors were used to report four temperature measurements in each aisle, these sensors were installed 1.9 m above the raised floor at the following rack inlets: C1-2, C1-6, C2-3, C2-6, D1-3, D1-7, D2-3, and D2-7 (refer to Fig. 1 for locations of these racks within the data center facility). Furthermore, each set of test conditions was allowed to operate for an extended time to ensure that steady state conditions had been achieved for the test conditions listed in Table 3. CRAH units return air temperature using their internal temperature sensors were collected and reported. After that the data was collected over a 10-minute period and the listed values in the table are averaged over the steady state operation of the cooling units and hence the data center room over that period. According to the flowrate measurements, the flow hood was used to take these measurements manually.

A comparison between the CFD and the experimental results in terms of temperature and tile average flow delivery for aisles C and D is provided in Fig. 5. It was found that the average tile flow delivery predicted by the CFD showed a great consistency with the experiment, where the CFD results lied within one standard deviation from the experimental ones. With regards to the temperature measurements, the maximum

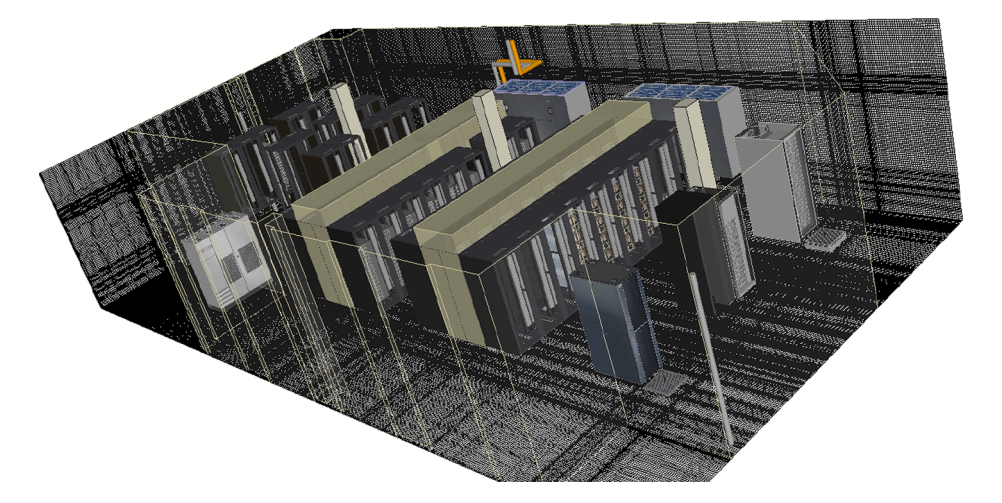


Fig. 4. Grid generation for the data center model.

**Table 3**Operating conditions for validation experiment.

Operating condition	Value
CRAH 1 SAT	10.4 °C
CRAH 1 fan speed	70%
CRAH 2 SAT	15.8 °C
CRAH 2 fan speed	100%
IT equipment utilization	Idling

mismatch between the CFD and the experiment was noticed to be 1.6  $^{\circ}$ C for rack D2-3. According to these results, the reliability, and the accuracy of this model in predicting both temperature field and tiles flowrate is confirmed. Finally, it is worth to mention that this model was developed for research purposes thus it has been tested against experimental results on many occasions considering various operating conditions, and it has proved it is validity in each time.

# • Partitions modeling

The flow of a fluid through a porous medium is described by Darcy's law, which represents the proportionality between the flow flux and the medium permeability, pressure drop, and the dynamic viscosity of the fluid. In the commercial CFD software used in this study, there are two methods to model the partitions. One way is to represent them as flow resistive medium, which requires to define and extract the flow resistance coefficients in all directions using manufacture's data of the object or to determine the inertia and viscous coefficients,  $k_1$  and  $k_2$ , respectively. Which also requires a knowledge of the P-Q curve as well.

$$\frac{\partial p}{\partial x_j} = \frac{1}{2} \rho V_j^2 \left[ k_1 + \frac{k_2}{V_j} \right] \tag{6}$$

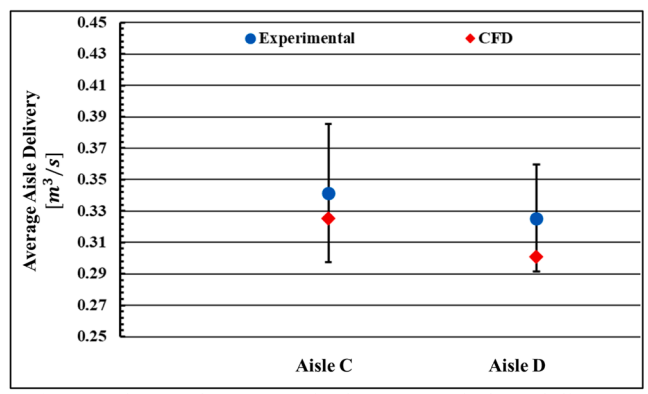
$$Porosity = \frac{Volume \ of \ voids}{Total \ volume} \tag{7}$$

The second is by defining the porosity in each spatial coordinate. For simplicity and generalization the results from this study the authors adapt the second method to model partitions by.

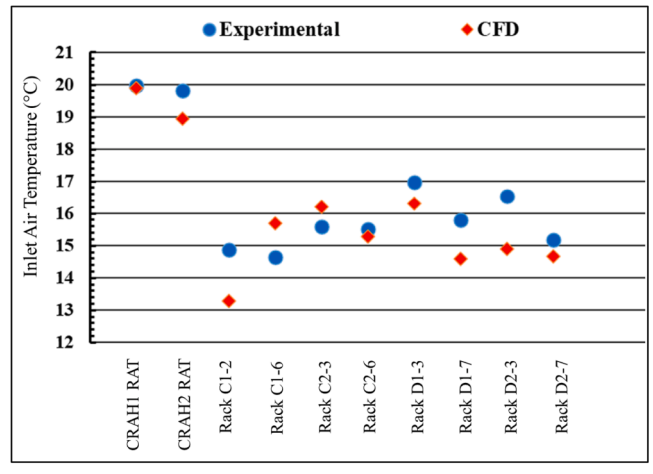
# 3. Results and discussion

## 3.1. Experimental results

As mentioned, the experiments were divided into four scenarios. The flowrate measurements for perforated tiles in aisles C and D collected from scenario 1 and 2 were compared with each other to show the effect



(a) Experimental vs numerical average airflow delivery of aisles C and D.



(b) Experimental vs numerical temperature measurements reported atselected racks and intake side of the cooling units.

Fig. 5. Comparison of airflow delivery and air temperature between experimental and numerical data.

of partitions on the flowrate distribution when both CRAH units operated together. The same was done for scenario 3 and 4 to illustrate the impact of using partitions when only CRAH 2 was on duty. The motive for inspecting scenario 3 and 4 arose from a previous experiment, which

showed that the effect of vortices was maximized when only one CRAH unit was on duty. In scenarios 1 and 2, the interaction of the CRAH units' flow prevented a vortex from forming under aisle C. However, there was no effect of the partitions on aisles A and E whereas the average tiles delivery was  $0.322\ (m^3/s)$  and  $0.144\ (m^3/s)$  respectively with and without partitions for scenarios 1 and 2. Whilst the average airflow for scenarios 3 and 4 in aisle A and E was  $0.17\ (m^3/s)$  and  $0.07\ (m^3/s)$ , respectively.

According to Appendix A, aisles C and D had two types of perforated tiles. The first type had an OAR of 22% while the second type had an OAR of 60%. To conduct a more representative comparison between the different scenarios, the flowrate results for tiles with the same OAR from each aisle were introduced.

The goal of using partitions was to improve the airflow uniformity in the aisle by influencing the pressure distribution and preventing vortices in the plenum under the cold aisle. In scenario 2, the interaction between the CRAH units prevented vortices from forming under aisle C, which means that using the partitions slightly improved airflow uniformity in scenario 2, as illustrated in Fig. 6. However, the figure shows that the tiles in aisle C that were closer to the cooling unit delivered a lower flow rate. This can be attributed to the high airflow velocity of CRAH 1, which shoots the flow horizontally under aisle C. A more in-depth discussion of the flow field in the plenum is provided in the following numerical simulation section.

Fig. 7 shows a comparison of scenario 4 with scenario 3 which illustrates the partitions' capability in preventing vortices and improving the flow uniformity. Statistical analyses that compare scenario 1 with scenario 2, and scenario 3 with 4 are summarized in Table 4. Since the standard deviation is intrinsically linked with the uniformity, it was adapted to give an indication of the flow delivery uniformity. The table shows that installing the partitions increased the flow delivery uniformity of the tiles within both aisles. Results were reported for the 22% and 60% OAR tiles in both aisles individually. Tiles with a 60% OAR witnessed a higher decrement in the standard deviation as their flowrate is more likely to be affected by the pressure distribution in the plenum. Furthermore, the partitions guided more flow into the tiles that were delivering the lowest flowrates. By implementing the partitions, the minimum flowrate delivered by the 22% OAR tile increased at least by 0.01 (m<sup>3</sup>/s) in scenarios 2 and 4, whilst the minimum flowrate delivered by the 60% OAR tile increased at least by 0.03 (m<sup>3</sup>/s) considering the same scenarios.

From Table 4 it can be inferred that the advantages of installing the partitions were not limited to improving airflow uniformity, but also included increasing the total flowrate delivered to aisles C and D without affecting the other aisles in the data center (aisles A and E). For all cases when both CRAH units were on duty, the flowrate increased from 15.351  $(m^3/s)$  to 15.528  $(m^3/s)$ , whereas the flowrate rose from 7.615  $(m^3/s)$  to 7.926  $(m^3/s)$  when CRAH 1 was turned off. These results suggest that enhancing the pressure distribution in the plenum reduced the cold air leakage from the plenum to room space through the raised floor, which in turn improved the overall cooling performance of the data center.

#### 3.2. Flowrate uniformity evaluation

Fig. 8 illustrates the variation plots of ten consecutive tile airflow measurements for scenarios 3 and 4 within a time laps of 15 s between each successive measurement. The variation plots clearly shows that the variation in tiles airflow was significantly reduced for scenario 4 compared to scenario 3 for both aisles C and D. Whilst, the reduction values vary among spatial location of the tile and the OAR as well. It can be inferred that tiles c5, c13, c2 and c15 have the highest variation amongst aisle C tiles for scenario 3. Whereby, similar trend was noticed for aisle D tiles. Moreover, the overall variations were reduced for most of the tiles in both aisles.

Furthermore, a uniformity index was defined in this study to quantify the benefit of partitions on the airflow uniformity. The above-mentioned 10 consecutive measurements were used to calculate the range of flow rate measurements for each tile that was used to calculate Flow Uniformity Index (FUI) as defined in Eqs. (8) and (9). Positive values of FUI indicates the variation is reduced in tiles airflow delivery through different scenarios. While negative values indicate additional variation introduced.

$$FUI_{tile,i} = \left[ \frac{Range_{tile,i}^{scenario \ 3} - Range_{tile,i}^{scenario \ 4}}{Range_{tile,i}^{scenario \ 3}} \right] \times 100\%$$
 (8)

$$Range_{tile,i}^{scenario,j} = [Maximum \ airflow \ rate - Minimum \ airflow \ rate]_{tile,i}^{scenario,j}$$
(9)

An illustration of the benefits of partitions addition in legacy data centers on the airflow uniformity is shown in Fig. 9. Results of FUI were reported for 22% and 60% OAR tiles in aisle C individually owing to the fact that the numerical model showed the vortex was under aisle C as illustrated in Fig. 10. It can be inferred that the partitions significantly improve the airflow uniformity within individual aisles and hence the facility. Aisle C tiles with 22% and 60% OAR have an average FUI of 40% and 32%, respectively.

# 3.3. Numerical results

#### • Partitions' effect on the flow distribution in the plenum

Airflow distribution within the plenum is complicated since the unguided pathways often result in unintended turbulences and vortices. Therefore, the CFD model was utilized to visualize the flow field inside the plenum. Fig. 10 (a) shows the flow pattern inside the plenum for Scenario 3. CRAH 2 had three radial fans that blew air in all directions, with most of the flow going under aisle C. The velocity streamlines clearly display two vortices centered in locations 1 and 2. These vortices and turbulences limited the perforated tiles cooling capacity and wasted cooling energy.

To illustrate how these partitions work, the CFD model was also used to depict the impact of installing the partitions on the flow and pressure fields. The CFD data center model was modified to include partitions under aisles C and D. Those partitions were adjusted to match the ones used in the experimental setup. It can be seen in Fig. 10 (b) that deploying the partitions prevented vortices from forming where they previously did in locations 1 and 2. In addition to preventing vortices, the partitions reduced the airflow speed under Aisle C by inaugurating an impedance to the CRAH 2 airflow jet under Aisle C. The plenum pressure may drop below cold aisle containment pressure in certain regions due the large velocities caused by the CRAH flow jet or vortices. Consequently, this forms a negative pressure difference through the perforated tiles. In such cases, downward flow or so called "backflow" occurs through the perforated tiles. Backflow will reduce the tiles' cooling capacity, which in turn means the adjacent racks will be insufficiently cooled.

The impact of the partitions, which prevented vortices and reduced airflow jet speed, is reflected in the pressure difference through the perforated tiles. Fig. 11 shows the pressure difference across all tiles with and without the partitions installed. Implementing partitions improved the pressure difference uniformity along the aisle as well as the tile itself.

Fig. 11 shows that tiles c2 and c6 had the highest negative pressure differential, exhibiting 0.04 and 0.029  $(m^3/s)$  of downward flow, respectively. After deploying the partitions, the amount of downward flow in tiles c2 and c6 decreased to 0.015 and 0.006  $(m^3/s)$ , respectively. Even though tile c4 lies withing the same region, it did not experience a negative pressure differential. This can be attributed to the low OAR of that tile since the pressure differential across the tile depends on OAR. In

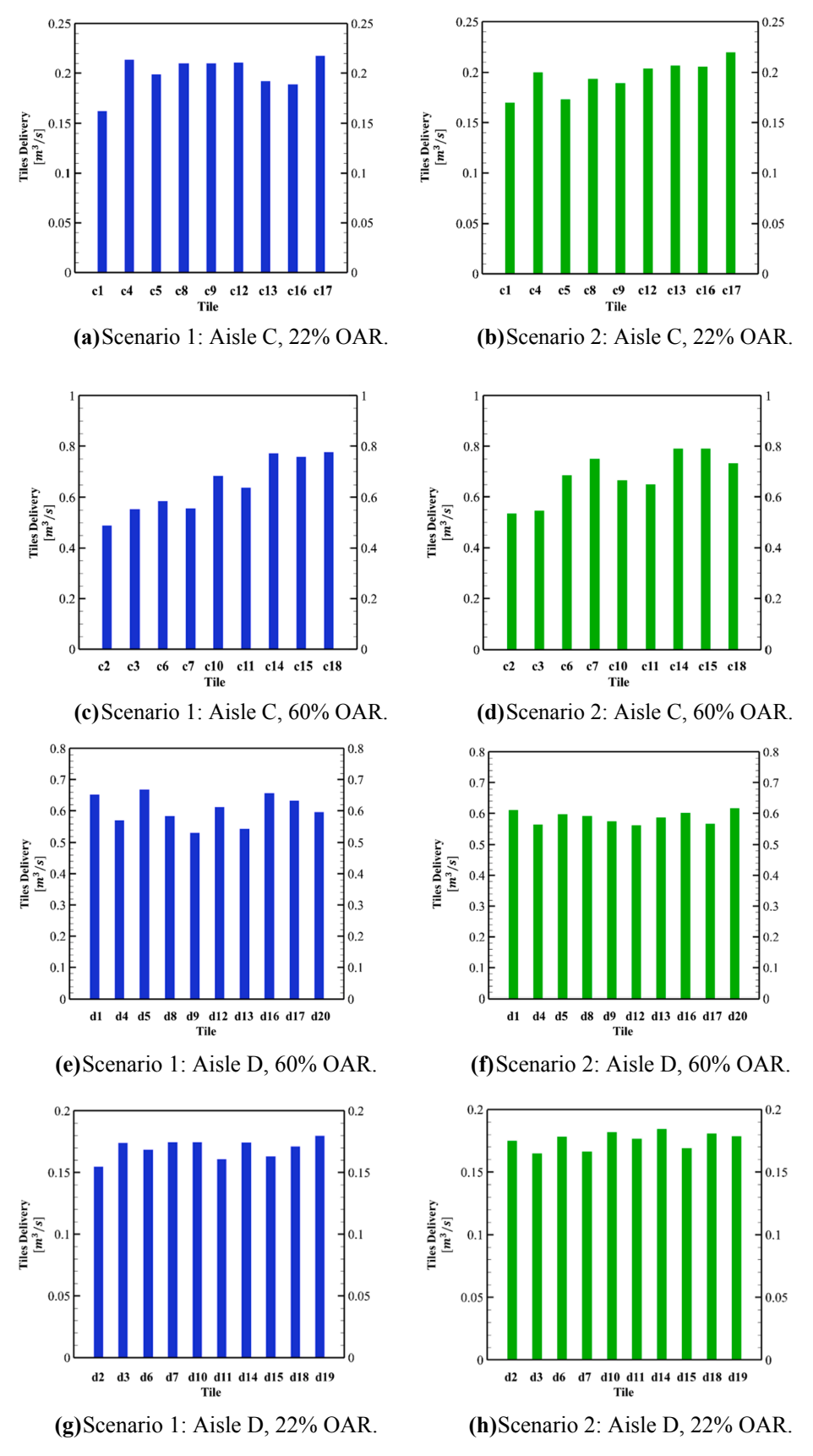


Fig. 6. Tiles airflow distribution in aisles C and D for scenarios 1 and 2.

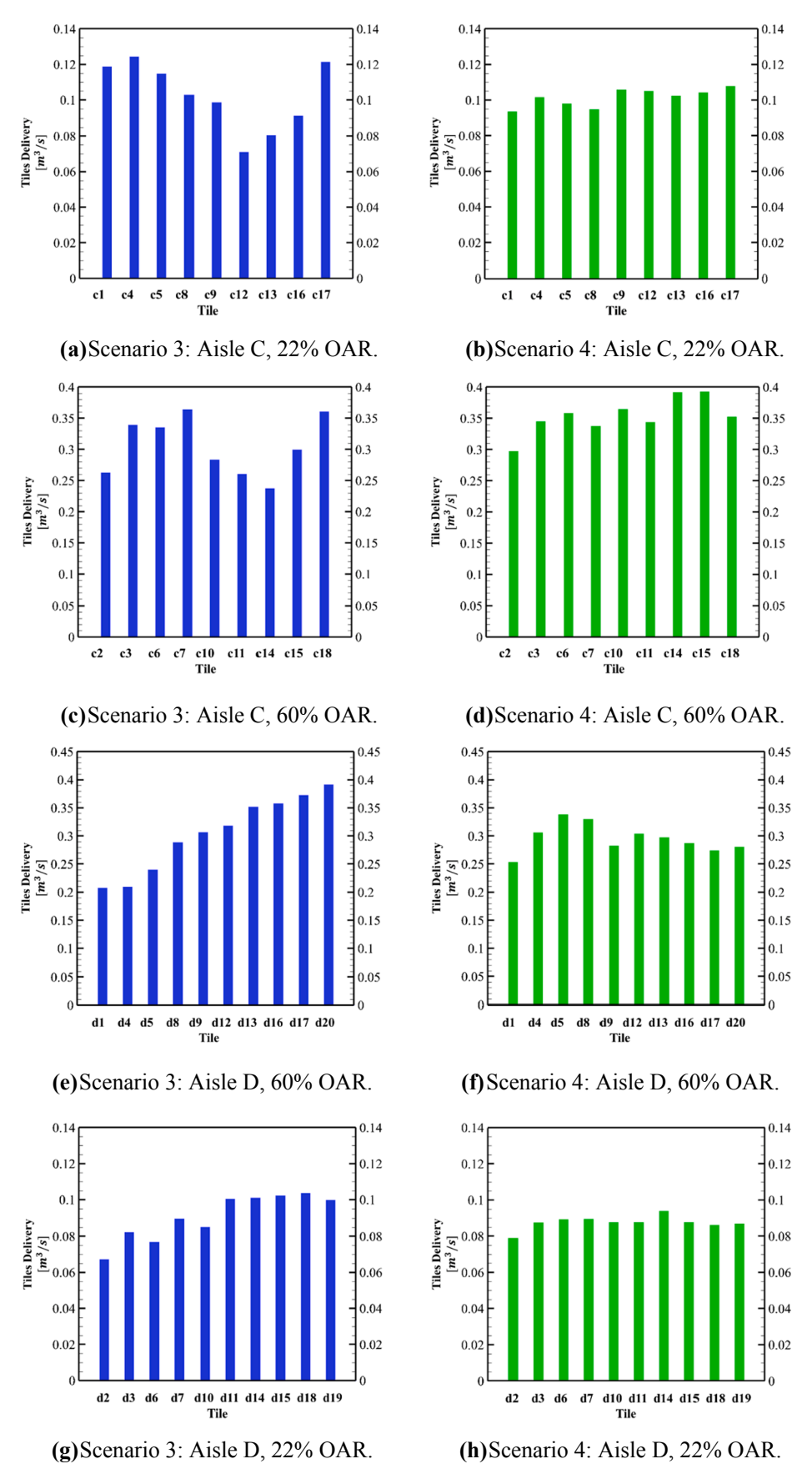


Fig. 7. Tiles airflow distribution in aisles C and D for scenarios 3 and 4.

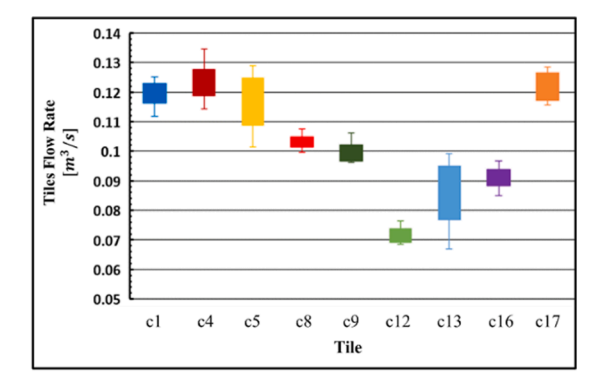
 Table 4

 Detailed statistical analysis for the tiles flow delivery.

	Scenario	22% OAR	22% OAR			60% OAR			
		1	2	3	4	1	2	3	4
Aisle C	<b>Sum</b> (m <sup>3</sup> /s)	1.803	1.761	0.92	0.914	5.808	6.145	2.743	3.183
	Average (m <sup>3</sup> /s)	0.2	0.196	0.103	0.102	0.645	0.683	0.305	0.354
	$Min (m^3/s)$	0.16	0.17	0.071	0.094	0.488	0.534	0.238	0.297
	$Max (m^3/s)$	0.217	0.219	0.124	0.108	0.776	0.791	0.364	0.393
	STD	0.017	0.016	0.019	0.005	0.107	0.095	0.047	0.029
Aisle D	$Sum (m^3/s)$	1.695	1.755	0.908	0.875	6.045	5.867	3.044	2.954
	Average (m <sup>3</sup> /s)	0.169	0.176	0.091	0.087	0.604	0.587	0.304	0.295
	$Min (m^3/s)$	0.155	0.165	0.067	0.079	0.531	0.561	0.208	0.254
	$Max (m^3/s)$	0.18	0.184	0.104	0.094	0.669	0.616	0.391	0.338
	STD	0.008	0.007	0.013	0.004	0.048	0.02	0.067	0.025

0.14

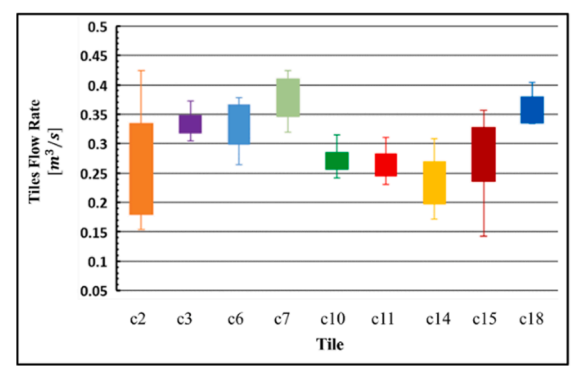
0.13

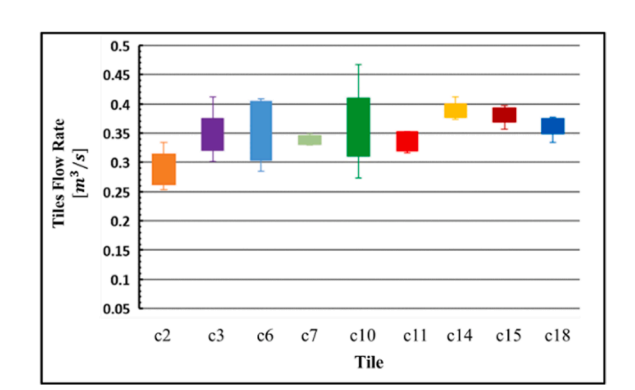


0.12 0.11 0.09 0.08 0.07 0.06 0.05 c1 c4 c5 c8 c9 c12 c13 c16 c17 Tile

(a) Scenario 3: Aisle C, 22% OAR tiles flow rate variation plot.

(b) Scenario 4: Aisle C, 22% OAR tiles flow rate variation plot.





(c) Scenario 3: Aisle C, 60% OAR tiles flow rate variation plot.

(d) Scenario 4: Aisle C, 60% OAR tiles flow rate variation plot.

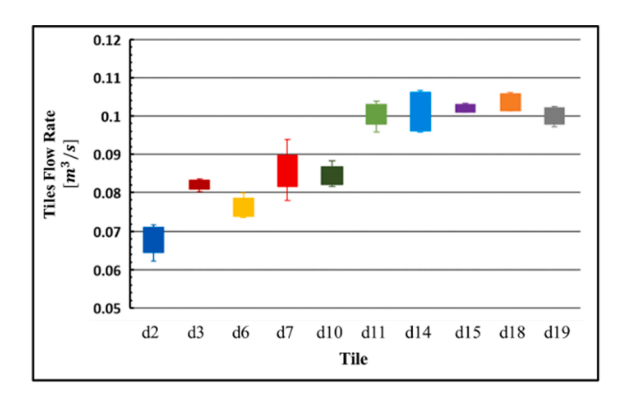
Fig. 8. Tiles flow measurement variation plots in aisles C and D for scenarios 3 and 4.

this case, the low OAR of this tile prevented the formation of downward flow across it. Fig. 12 shows an example of the downward flow in tile c2 considering scenario 3.

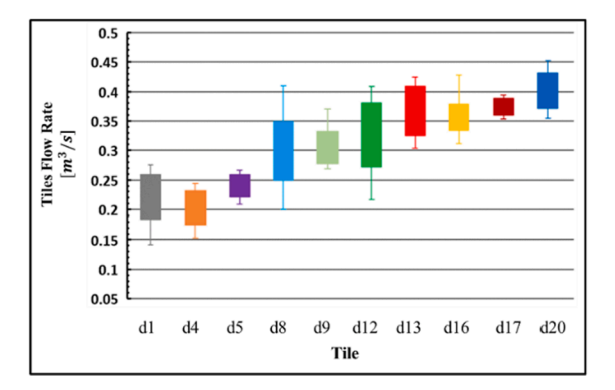
Following the investigation of the flow and pressure fields was the investigation of the partitions' impact on thermal distribution. The maldistribution of perforated tiles airflow delivery creates a nonuniform cooling distribution. Therefore, improving the flow field uniformity should increase airflow delivery to IT equipment that have experienced a lack of cool air. Fig. 13 shows the average inlet temperature for IT equipment in aisle C and D. The rows can be identified by referring to

Fig. 1 and the cabinets are numbered from left to the right. In Fig. 13, white is used to depict the IT equipment that were powered off during the experiment.

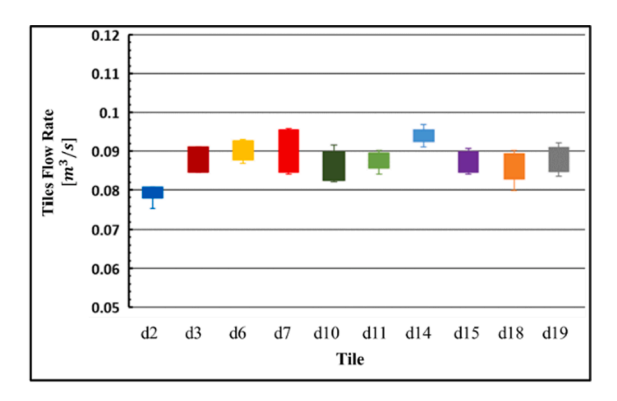
Fig. 13 shows that installing the partitions enhanced the cool airflow delivery for almost all racks. For row C1, the overall row exhibited a better cool airflow supply, which can be noticed by comparing the mean inlet temperature entering the switches at the top of the racks. Generally, these switches have weak fans. Since they are commonly placed at the top of the racks, they are more likely to be exposed to insufficient flow delivery. In row C1, all of the IT equipment inlet temperatures were



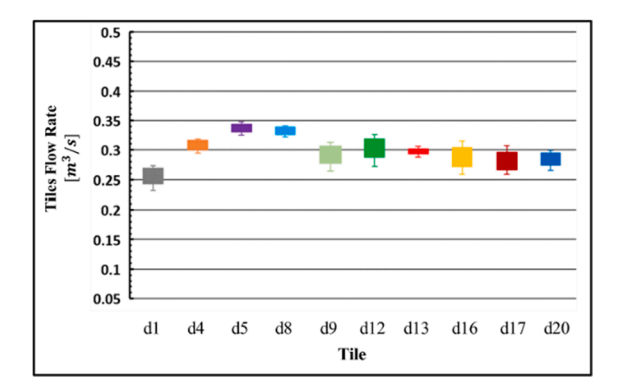
(e) Scenario 3: Aisle D, 22% OAR tiles flow rate variation plot.



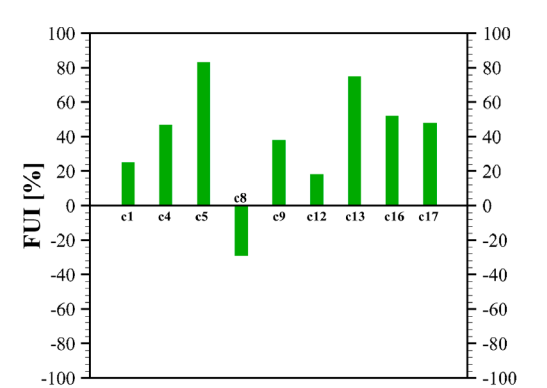
(g) Scenario 3: Aisle D, 60% OAR tiles flow rate variation plot.



(f) Scenario 4: Aisle D, 22% OAR tiles flow rate variation plot.



(e) Scenario 4: Aisle D, 60% OAR tiles flow rate variation plot.



100 100 80 80 60 60 40 40 20 20 0 -20 -40 -40 -60 -60 -80 -80 -100

Fig. 9. Flow uniformity indices (%) for aisles C and D for scenarios 3 and 4.

Fig. 8. (continued).

within the zone recommended by the ASHRAE thermal guidelines [48], except for the switches in racks C1-7 and C1-8, which experienced an average inlet temperature of 28.8  $^{\circ}$ C and 29.6  $^{\circ}$ C, respectively.

Row C2 endured a low cool air supply, hence IT equipment in various racks experienced an elevated mean inlet temperature. The deployment of partitions solved this issue for most racks, excluding racks C2-1 and C2-2, which contained a high IT power load. Improving the airflow delivery uniformity did not have a major impact on aisle D, seeing as this aisle was not affected by the unintended turbulences and vortices. The most significant change in this aisle was introduced by the blade center located at rack D2-3, where the mean inlet temperature increased from  $28.1\ ^{\circ}\text{C}$  to  $28.7\ ^{\circ}\text{C}$ .

Note that high IT equipment inlet temperature should be avoided in an actual data center, since it will impact reliability [49]. In this study, the experiment was conducted for a limited time for research purposes to highlight the potential of employing partitions. The data center room temperature and CPU temperatures were monitored during the experiment to make sure that no harm came to any of the IT equipment.

# • Partitions' geometrical parametric study

To quantify the effects of partition geometry, 36 CFD models were solved considering the various geometrical parameters of partitions. Three different heights (304.8 mm, 609.8 mm, 914.4 mm) with three

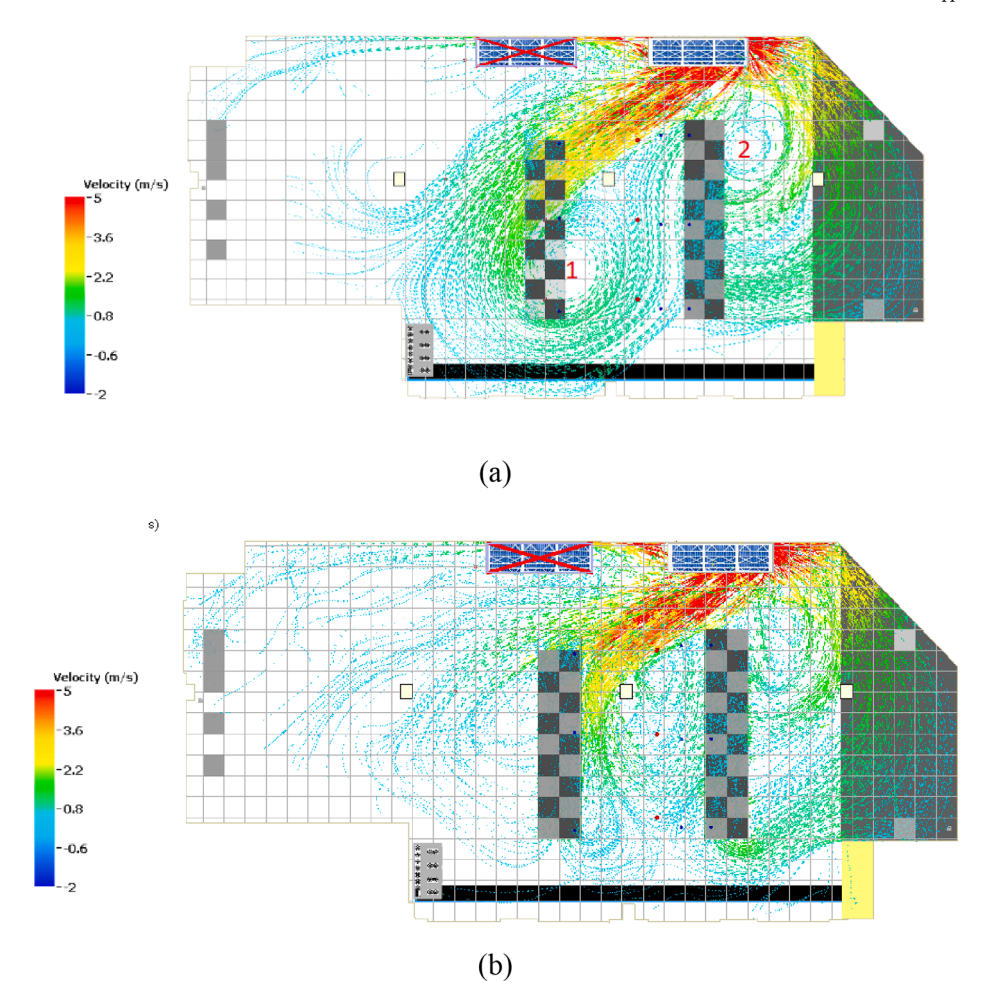


Fig. 10. Underfloor airflow velocity streamlines. (a) Scenario 3. (b) Scenario 4.

different widths (10 mm, 50 mm, 100 mm)were analyzed. Three different partition porosities (0%, 25%, 50%, 75%) were investigated. Table 5 shows the parameters of all those cases. CRAH 1 remained shut down while CRAH 2 was kept powered on at full cooling capacity. Plenum height, perforated tile OAR, and all other variables of the data center were kept unchanged.

Partition geometry was compared based on three different performance factors: SHI, percentage of IT that exceeded the ASHRAE recommended SAT, and raised floor leakage as a percentage of total flowrate delivered. The used software in this study gives the option to specify the gap in the raised floor. The measured raised floor gap for ES2 data center laboratory imposed in the CFD model. Then, the model reported the leakage through the raised floor seems and pluming holes based on the specified gap size.

Although the Power Usage Effectiveness (PUE) is one of the most common efficiency metrics for DC efficiency. In simple terms, PUE is the ratio of power delivered to the facility divided by the power delivered to servers, storage, and networking gear. The PUE represented in equation shown below, represents a ratio between the total facility power (total IT, chiller, blower, and lighting power) and the total IT equipment power.

$$PUE = \frac{IT\ power + Blowers + Chiller + Lighting}{IT\ Equipment\ Power}$$

One of the issues with the PUE metric is the inclusion of server fan power in the total IT equipment power. Occasionally and to save energy at the cooling infrastructure level by raising the cooling equipment set point it may in some cases cause an increase in server's fan power, thereby increasing the total IT equipment power. The PUE metric however would not capture this effect and would always show a lower PUE number. Whereas SHI was introduced by Sharma et al. [50]. The advantage of this index is that it can be used as a tool to investigate convective heat transfer and improve energy efficiency. Furthermore, it is scalable and can be applied at the rack, row, and data center level l. SHI indicates the amount of heat that infiltrates the cold aisle and eventually gets pulled into the equipment that produces heat. The SHI is calculated using the ratio of the enthalpy rise in the cold aisle caused by the infiltration to the total enthalpy rise through the rack [51]. Subsequently and based on the definition of SHI. Decreasing the SHI will improve the overall thermal performance of the cooling system. In addition, an energy saving was gained by reducing the amount of cold air losses as well as reducing the air temperature at the intake of the IT equipment which in turn leads to reduce the air mixing between hot and cold aisles.

$$SHI = \frac{\Delta \dot{Q}^{CA}}{\dot{Q} + \Delta \dot{Q}^{CA}} \tag{10}$$

where,  $\Delta \dot{Q}^{CA}$  is the enthalpy increase caused by infiltration and  $\dot{Q}$  is the total heat dissipated by the IT equipment. Based on the above, decreasing the SHI will improve the overall thermal performance of the cooling system. Results for the partitions' geometrical parametric study are summarized in Table 6.

In Table 6, the baseline case represents the case without any partitions employed. Based on the results, partitions were beneficial or detrimental depending on their geometry. For example, when the partition height equaled 914.4 mm, which was the full height of the

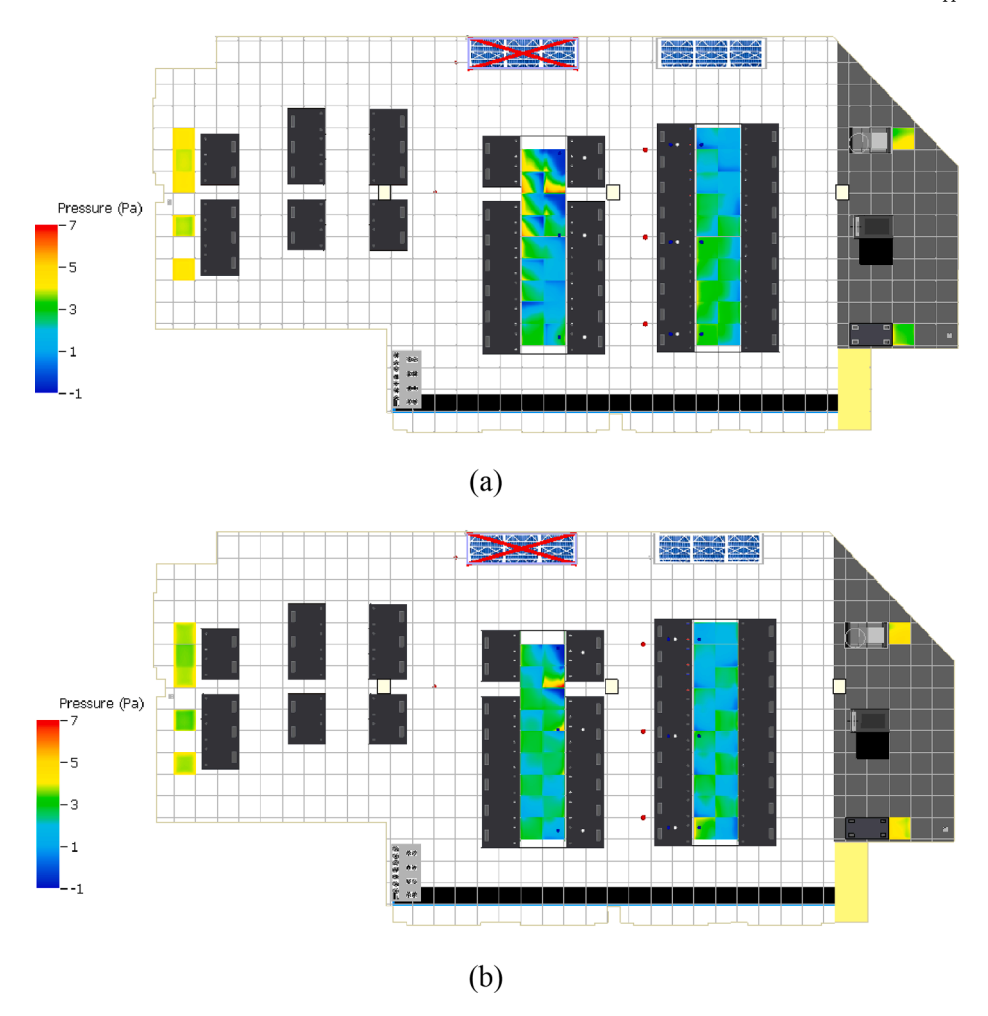


Fig. 11. Pressure distribution in plenum under tiles in aisles C and D. (a) Scenario 3. (b) Scenario 4..

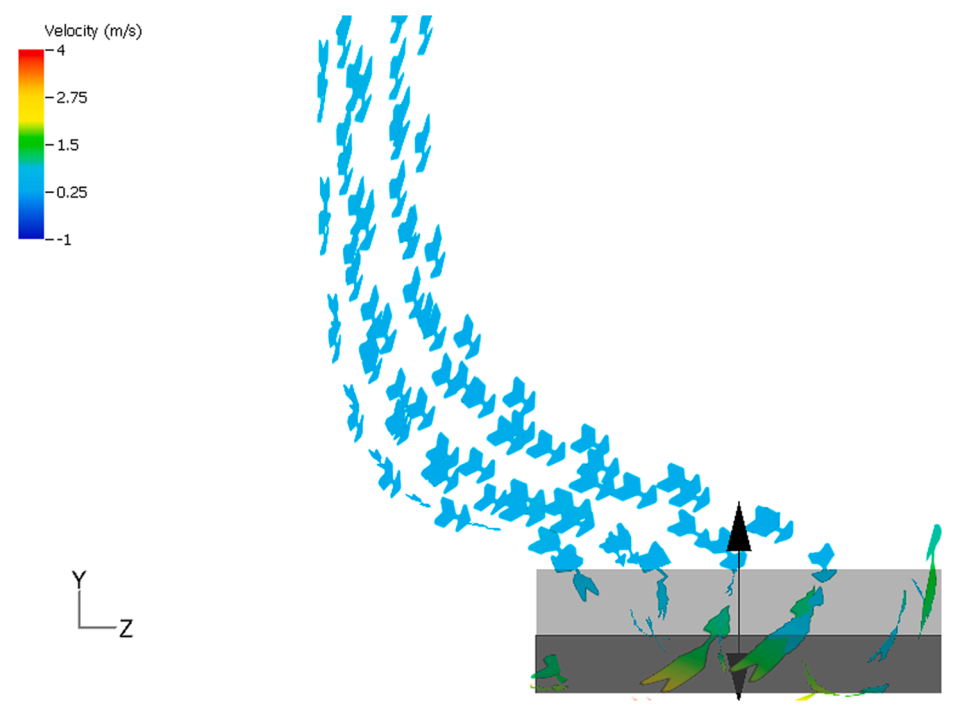


Fig. 12. Down flow in tile c2.

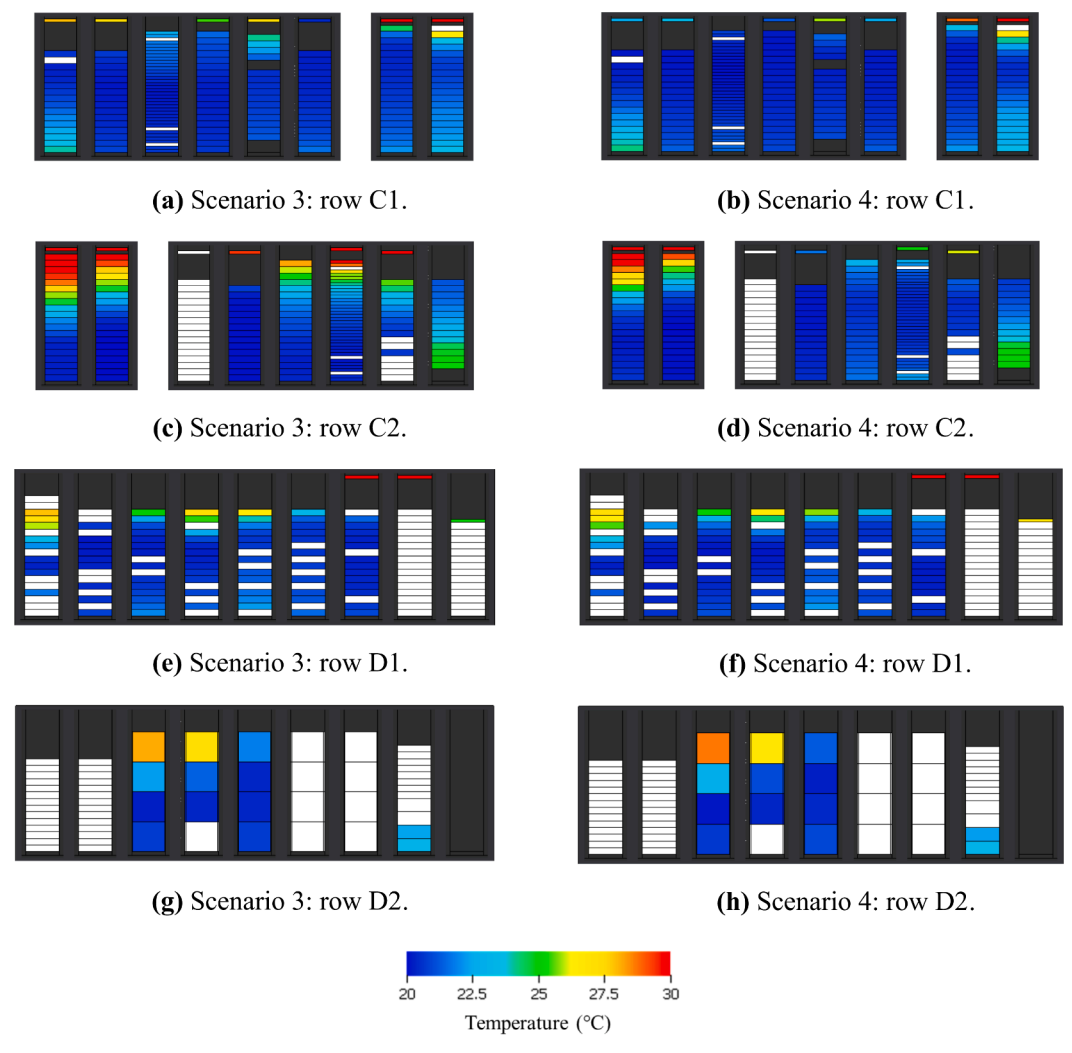


Fig. 13. Mean inlet temperature for IT equipment.

**Table 5**Geometrical partitions' parameters.

Cases	Partition height (mm)	Partition width (mm)	Partion porosity %
1,2,3	304.8, 609.8, 914.4	10	0
4,5,6	304.8, 609.8, 914.4	50	0
7,8,9	304.8, 609.8, 914.4	100	0
10,11,12	304.8, 609.8, 914.4	10	25
13,14,15	304.8, 609.8, 914.4	50	25
16,17,18	304.8, 609.8, 914.4	100	25
19,20,21	304.8, 609.8, 914.4	10	50
22,23,24	304.8, 609.8, 914.4	50	50
25,26,27	304.8, 609.8, 914.4	100	50
28,29,30	304.8, 609.8, 914.4	10	75
31,32,33	304.8, 609.8, 914.4	50	75
34,35,36	304.8, 609.8, 914.4	100	75

plenum, both the SHI increased and the leakage percentage increased. Thus, the cooling system's performance degraded, and more hot air infiltrated the cold aisle. This can be attributed to the partition blocking most of the air from entering the cold aisle from the sides, except for in cases 12, 21, and 30.

In these three cases, the partitions were thin and porous enough to allow air to penetrate the cold aisle from the sides. Increasing partition porosity improved the overall cooling system performance, while increasing the wall width degraded the overall cooling system performance.

Considering the 304.8 and 609.8 partition heights, for all cases the cooling system performance was enhanced with respect to all three performance aspects. Overall, no pattern was found to directly correlate any of the geometrical parameters to performance.

With respect to the SHI, case 28 featured the lowest value of 0.177. However, this case did not represent the best point in terms of the percentage of IT that exceeded the ASHRAE recommended SAT and leakage. Looking at the partition geometry of all the cases, case 20 would provide the best compromise between the three performance aspects, since it had the lowest amount of leakage, lowest percentage of IT with an elevated SAT, and a relatively low SHI. By adopting these geometrical parameters, the SHI by 10.4%, the percentage of IT equipment violating ASHRAE recommendation decreased from 7.5% to 4.668%, and the leakage decreased from 2.51% to 1.15%. In the future, genetic algorithms could be developed to further analyze the optimal partition design.

## 4. Conclusions

This study proposed and experimentally verified a novel approach using easily adoptable porous partitions deployed in the plenum of existing and future data centers. The results of the experimental and numerical investigation of partitions influence on the thermal performance of the data center for different operating conditions can be summarized as follows:

**Table 6**Geometrical parameters for installed partitions.

Cases	SHI	Equipment over ASHRAE %	Leakage %	Cases	SHI	Equipment over ASHRAE %	Leakage %
Baseline	0.202	7.5	2.51	19	0.179	5.49	1.21
1	0.18	5.45	1.21	20	0.181	4.67	1.15
2	0.199	7.76	1.35	21	0.188	4.86	1.20
3	0.216	9.86	2.94	22	0.178	5.71	1.17
4	0.178	5.71	1.17	23	0.194	6.93	1.33
5	0.195	6.93	1.35	24	0.217	8.82	2.57
6	0.222	11.20	2.84	25	0.178	5.38	1.17
7	0.178	5.38	1.17	26	0.194	6.93	1.34
8	0.195	6.93	1.35	27	0.212	8.49	2.70
9	0.215	8.82	2.83	28	0.177	5.49	1.22
10	0.18	5.45	1.20	29	0.178	4.96	1.17
11	0.19	5.17	1.22	30	0.179	4.87	1.17
12	0.203	7.72	1.53	31	0.178	5.71	1.17
13	0.178	5.71	1.17	32	0.194	6.93	1.34
14	0.195	6.93	1.34	33	0.215	8.03	2.46
15	0.22	8.82	2.69	34	0.178	5.38	1.17
16	0.178	5.38	1.17	35	0.194	6.93	1.33
17	0.195	6.93	1.34	36	0.212	8.35	2.64
18	0.214	8.82	2.76				

- Deploying the novel partitions significantly improved tiles airflow uniformity through the elimination of the sources of flow maldistribution such as vortices under aisle C.
- The introduced flow uniformity index (FUI) indicated that the tiles air delivery variation was reduced with installed partitions. Aisle C with 22% and 60% OAR have an average FUI of 40% and 32%, respectively. Whereas the FUI average for aisle D tiles with 60% OAR was 60%.
- $\bullet$  The partitions decreased the tiles backflow from 0.04 to 0.015  $(m^3/s)$  and from 0.029 to 0.006  $(m^3/s)$  which counts for 62% and 79% reduction for tiles c2 and c6, respectively.
- As a measure related to hot air recirculation and one of the performance metrics in data centers. The SHI was decreased by 10% for scenario 3 over scenario 4.
- The number of IT equipment that violates the guidelines by ASHRAE for the recommended inlet air temperature was reduced by 40% with partitions in place. Moreover, the results showed a reduction in IT equipment air inlet temperature by 2–5 °C at specific spatial planes for scenario 4 among 3. And hence suppress the chances of hot spots formation in the cold aisle.
- The partitions influence was not limited to improve airflow uniformity, but also included increasing the total flowrate delivered to aisles C and D without affecting the other aisles in the data center (aisles A and E). For all cases when both CRAH units were on duty, the flowrate increased from 15.351 (m³/s) to 15.528 (m³/s), whereas the flowrate rose from 7.615 (m³/s) to 7.926 (m³/s) when CRAH 1 was turned off. These results suggest that enhancing the pressure distribution in the plenum reduced the cold air leakage from the plenum to room space through the raised floor, which in turn improved the overall cooling performance of the data center

Finally, the partitions geometrical parameters, including height,

width, and porosity, were investigated. Results showed that using partitions with the following geometry had the most beneficial impact: 609.8~(mm)height, 10~(mm) width, and 50% porosity. It was found that the SHI decreased by 10.4%, the percentage of IT equipment violating the ASHRAE recommendations in terms of hardware air inlet temperature decreased from 7.5% to 4.668%, and the leakage decreased from 2.51% to 1.15%.

# CRediT authorship contribution statement

Mohammad I. Tradat: Conceptualization, Investigation, Methodology, Data curation, Formal analysis, Resources, Software, Validation, Visualization, Writing - original draft. Yaman "Mohammad Ali" Manaserh: Investigation, Data curation, Formal analysis, Software, Validation, Visualization, Writing - original draft. Bahgat G. Sammakia: Conceptualization, Supervision, Writing - review & editing. Cong Hiep Hoang: Writing - review & editing. Husam A. Alissa: Supervision, Writing - review & editing.

#### **Declaration of Competing Interest**

The authors declare that they have no known competing financial interests or personal relationships that could have appeared to influence the work reported in this paper.

## Acknowledgements

We would like to acknowledge Future Facilities Ltd. We would also like to thank the ES2 Partner Universities for their support and advice. This work is supported by NSF IUCRC Award No. IIP- 1738793 and MRI Award No. CNS1040666.

Appendix A. Data center specifications and operating conditions

Aisle	Cabinet	Value	Perforated tile	OAR
A	A 1–1	4.54	a1	22
	A 1–2	4.436	a2	32
	A 1–3	0	a3	22
	A 1–4	0	a4	32
	A 1–5	0	a5	22
С	C 1–1	2.2	c1	22
			Continu	od on nost nago)

(continued on next page)

M.I. Tradat et al.

#### (continued)

Aisle	Cabinet	Value	Perforated tile	OAR
	C 1–2	2.2	c2	60
	C 1–3	2.35	c3	60
	C 1–4	1.8	c4	22
	C 1–5	2.3	c5	22
	C 1–6	2.88	c6	60
	C 1–7	2.97	c7	60
	C 1–8	2.43	c8	22
	C 2–1	2.2	c9	22
	C 2–2	2.2	c10	60
	C 2–3	0	c11	60
	C 2-4	1.8	c12	22
	C 2–5	2.2	c13	22
	C 2–6	10.9	c14	60
	C 2–7	10.9	c15	60
	C 2-8	2.5	c16	22
			c17	22
			c18	60
D	D 1–1	3.42	d1	60
	D 1–2	4.25	d2	22
	D 1-3	4.25	d3	22
	D 1-4	4.16	d4	60
	D 1-5	4.25	d5	60
	D 1-6	4.16	d6	22
	D 1–7	4.25	d7	22
	D 1-8	4.16	d8	60
	D 1-9	3.42	d9	60
	D 2-1	0.09	d10	22
	D 2-2	0	d11	22
	D 2-3	4	d12	60
	D 2-4	4	d13	60
	D 2-5	4	d14	22
	D 2-6	4	d15	22
	D 2-7	0	d16	60
	D 2-8	0	d17	60
	D 2-9	0	d18	22
			d19	22
			d20	60
E	E1-1	0	e1	60

#### References

- [1] Ahmad AD, Abubaker AM, Najjar YS, Manaserh YMA. Power boosting of a combined cycle power plant in Jordan: An integration of hybrid inlet cooling & solar systems. Energy Convers Manage 2020;214:112894.
- [2] Tradat M, Mohsenian G, Manaserh Y, Sammakia B, Mendo D, Alissa HA. Experimental analysis of different measurement techniques of server-rack airflow predictions towards proper DC airflow management. In: 2020 19th IEEE Intersociety Conference on Thermal and Thermomechanical Phenomena in Electronic Systems (ITherm): IEEE; 2020. p. 366–73.
- [3] Deymi-Dashtebayaz M, Namanlo SV, Arabkoohsar A. Simultaneous use of air-side and water-side economizers with the air source heat pump in a data center for cooling and heating production. Appl Therm Eng 2019;161:114133.
- [4] Manaserh YM, Tradat MI, Mohsenian G, Sammakia BG, Seymour MJ. General guidelines for commercialization a small-scale in-row cooled data center: a case study. In: 2020 36th Semiconductor Thermal Measurement, Modeling & Management Symposium (SEMI-THERM). IEEE; 2020. p. 48–55.
- [5] Ortega A, del Valle M, Caceres CVHTX. A code for simulation of steady state and dynamic response of single or multiple networked cross flow heat exchangers in data center thermal management systems. In: 2017 33rd Thermal Measurement, Modeling & Management Symposium (SEMI-THERM). IEEE; 2017. p. 88–94.
- [6] del Valle M, Caceres C, Ortega A. Transient modeling and validation of chilled water based cross flow heat exchangers for local on-demand cooling in data centers. In: 2016 15th IEEE Intersociety Conference on Thermal and Thermomechanical Phenomena in Electronic Systems (ITherm). IEEE; 2016. p. 727–36
- [7] Hoang CH, Khalili S, Ramakrisnan B, Rangarajan S, Hadad Y, Radmard V, et al. An experimental apparatus for two-phase cooling of high heat flux application using an impinging cold plate and dielectric coolant. In: 2020 36th Semiconductor Thermal Measurement, Modeling & Management Symposium (SEMI-THERM). IEEE; 2020. p. 32–8.
- [8] Caceres C, Ortega A, Wemhoff A, Jones GF. Numerical analysis of two phase cross-flow heat exchanger for high power density equipment in data centers under dynamic conditions. In: 2020 19th IEEE Intersociety Conference on Thermal and Thermomechanical Phenomena in Electronic Systems (ITherm). IEEE; 2020. p. 520–9.

[9] Cho J, Kim Y. Improving energy efficiency of dedicated cooling system and its contribution towards meeting an energy-optimized data center. Appl Energy 2016; 165:967–82.

Applied Energy 289 (2021) 116663

- [10] Tatchell-Evans M, Kapur N, Summers J, Thompson H, Oldham D. An experimental and theoretical investigation of the extent of bypass air within data centres employing aisle containment, and its impact on power consumption. Appl Energy 2017;186:457–69.
- [11] Fakhim B, Behnia M, Armfield S, Srinarayana N. Cooling solutions in an operational data centre: A case study. Appl Therm Eng 2011;31:2279–91.
- [12] Gupta R, Asgari S, Moazamigoodarzi H, Pal S, Puri IK. Cooling architecture selection for air-cooled Data Centers by minimizing exergy destruction. Energy 2020:117625.
- [13] Silva-Llanca L, Ortega A, Fouladi K, del Valle M, Sundaralingam V. Determining wasted energy in the airside of a perimeter-cooled data center via direct computation of the Exergy Destruction. Appl Energy 2018;213:235–46.
- [14] Yuan X, Xu X, Wang Y, Liu J, Kosonen R, Cai H. Design and validation of an airflow management system in data center with tilted server placement. Appl Therm Eng 2020;164:114444.
- [15] Liu Y, Ma G, Xue L, Zhou F, Wang L. Energy-saving effect of integrated cooling unit with rotary booster and compressor for data center. Int J Refrig 2020.
- [16] Cheung H, Wang S, Zhuang C, Gu J. A simplified power consumption model of information technology (IT) equipment in data centers for energy system real-time dynamic simulation. Appl Energy 2018;222:329–42.
- [17] Li J, Jurasz J, Li H, Tao W-Q, Duan Y, Yan J. A new indicator for a fair comparison on the energy performance of data centers. Appl Energy 2020;276:115497.
- [18] Yuan X, Xu X, Liu J, Pan Y, Kosonen R, Gao Y. Improvement in airflow and temperature distribution with an in-rack UFAD system at a high-density data center. Build Environ 2020;168:106495.
- [19] Khalaj AH, Halgamuge SK. A Review on efficient thermal management of air-and liquid-cooled data centers: From chip to the cooling system. Appl Energy 2017;205: 1165–88
- [20] Lu H, Zhang Z, Yang L. A review on airflow distribution and management in data center. Energy Build 2018;179:264–77.
- [21] Jin C, Bai X, Yang C, Mao W, Xu X. A review of power consumption models of servers in data centers. Appl Energy 2020;265:114806.

- [22] Huang P, Copertaro B, Zhang X, Shen J, Löfgren I, Rönnelid M, et al. A review of data centers as prosumers in district energy systems: Renewable energy integration and waste heat reuse for district heating. Appl Energy 2020;258:114109.
- [23] Gong X, Zhang Z, Gan S, Niu B, Yang L, Xu H, et al. A review on evaluation metrics of thermal performance in data centers. Build Environ 2020:106907.
- [24] Shrivastava S, Sammakia B, Schmidt R, Iyengar M. Comparative analysis of different data center airflow management configurations. In: International Electronic Packaging Technical Conference and Exhibition; 2005. p. 329–36.
- [25] Khalili S, Tradat MI, Nemati K, Seymour M, Sammakia B. Impact of tile design on the thermal performance of open and enclosed aisles. J Electron Packag 2018;140.
- [26] Zhang M, Zhang Z, Hu Y, Geng Y, Huang H, Huang Y. Effect of raised floor height on different arrangement of under-floor air distribution performance in data center. Procedia Eng 2017;205:556–64.
- [27] Song Z. Thermal performance of a contained data center with fan-assisted perforations. Appl Therm Eng 2016;102:1175–84.
- [28] VanGilder JW, Schmidt RR. Airflow uniformity through perforated tiles in a raisedfloor data center. In: International Electronic Packaging Technical Conference and Exhibition; 2005. p. 493–501.
- [29] Bhopte S, Sammakia B, Iyengar M, Schmidt R. Numerical and experimental study of the effect of underfloor blockages on data center performance. J Electron Packag 2011;133
- [30] Bhopte S, Sammakia B, Iyengar MK, Schmidt R. Guidelines on managing under floor blockages for improved data center performance. In: ASME International Mechanical Engineering Congress and Exposition; 2006. p. 83–91.
- [31] Alissa H, Alkharabsheh S, Bhopte S, Sammakia B. Numerical investigation of underfloor obstructions in open-contained data center with fan curves. In: Fourteenth Intersociety Conference on Thermal and Thermomechanical Phenomena in Electronic Systems (ITherm). IEEE; 2014. p. 771–7.
- [32] Fulpagare Y, Mahamuni G, Bhargav A. Effect of plenum chamber obstructions on data center performance. Appl Therm Eng 2015;80:187–95.
- [33] Fakhim B, Srinarayana N, Behnia M, Armfield S. Effect of under-floor blockages and perforated tile openings on the performance of raised-floor data centres. 17th Australasian Fluid Mechanics Conference, 2010.
- [34] Patankar SV. Airflow and cooling in a data center. J Heat Transfer 2010;132.
- [35] Karki KC, Patankar SV, Radmehr A. Techniques for controlling airflow distribution in raised-floor data centers. In: International Electronic Packaging Technical Conference and Exhibition; 2003. p. 621–8.
- [36] Zhang Y, Zhang K, Liu J, Kosonen R, Yuan X. Airflow uniformity optimization for modular data center based on the constructal T-shaped underfloor air ducts. Appl Therm Eng 2019;155:489–500.

- [37] Yuan X, Liu J, Yang Y, Wang Y, Yuan X. Investigation and improvement of air distribution system's airflow performance in data centers. Procedia Eng 2017;205: 2895–902
- [38] Lu H, Zhang Z. Optimizing thermal performance of data centers with novel local partition configurations. In: IOP Conference Series: Earth and Environmental Science. IOP Publishing; 2018. p. 012068.
- [39] Lu H, Zhang Z. Numerical and experimental investigations on the thermal performance of a data center. Appl Therm Eng 2020;180:115759.
- [40] Tradat MI, Khalili S, Khatabi M, Sammakia BG, Seymour M, Tipton R, et al. Numerical Investigation of Novel Underfloor Air-Directors Effect on Data Center Performance. In: 2019 18th IEEE Intersociety Conference on Thermal and Thermomechanical Phenomena in Electronic Systems (ITherm). IEEE; 2019. p. 886–96
- [41] Conner ME, Baglietto E, Elmahdi AM. CFD methodology and validation for singlephase flow in PWR fuel assemblies. Nucl Eng Des 2010;240:2088–95.
- [42] Priyadumkol J, Kittichaikarn C. Application of the combined air-conditioning systems for energy conservation in data center. Energy Build 2014;68:580–6.
- [43] Almoli A, Thompson A, Kapur N, Summers J, Thompson H, Hannah G. Computational fluid dynamic investigation of liquid rack cooling in data centres. Appl Energy 2012;89:150–5.
- [44] Ling Y-Z, Zhang X-S, Zhang K, Jin X. On the characteristics of airflow through the perforated tiles for raised-floor data centers. J Build Eng 2017;10:60–8.
- [45] Lee J, Moshfeghi M, Choi Y, Hur N. A numerical simulation on recirculation phenomena of the plume generated by obstacles around a row of cooling towers. Appl Therm Eng 2014;72:10–9.
- [46] Huang M-H, Chen L, Lei L, He P, Cao J-J, He Y-L, et al. Experimental and numerical studies for applying hybrid solar chimney and photovoltaic system to the solarassisted air cleaning system. Appl Energy 2020;269:115150.
- [47] Calautit JK, Hughes BR, Nasir DS. Climatic analysis of a passive cooling technology for the built environment in hot countries. Appl Energy 2017;186:321–35.
- [48] 9.9 ATC. Thermal Guidelines for Data Processing Environments 4th ed. Atlanta: W. Stephen Comstock; 2015.
- [49] Manaserh YM, Tradat MI, Mohsenian G, Sammakia BG, Ortega A, Seymour MJ, et al. Novel Experimental Methodology for Characterizing Fan Performance in Highly Resistive Environments. In: 2020 19th IEEE Intersociety Conference on Thermal and Thermomechanical Phenomena in Electronic Systems (ITherm). IEEE; 2020. p. 1–7.
- [50] Sharma R, Bash C, Patel C. Dimensionless parameters for evaluation of thermal design and performance of large-scale data centers. In: 8th AIAA/ASME Joint Thermophysics and Heat Transfer Conference: 2002. p. 3091.
- [51] Capozzoli A, Serale G, Liuzzo L, Chinnici M. Thermal metrics for data centers: A critical review. Energy Procedia 2014;62:391–400.